Positron Lymphography via Intracervical ^{18}F-FDG Injection for Presurgical Lymphatic Mapping in Cervical and Endometrial Malignancies

Jennifer J. Mueller[1,2], Lawrence T. Dauer[3], Rajmohan Murali[4], Alexia Iasonos[5], Neeta Pandit-Taskar[6], Nadeem R. Abu-Rustum[1,2], and Jan Grimm[6–9]

[1]Gynecology Service, Department of Surgery, Memorial Sloan Kettering Cancer Center, New York, New York; [2]Department of Obstetrics and Gynecology, Weill Cornell Medical College, New York, New York; [3]Department of Radiology, Memorial Sloan Kettering Cancer Center, New York, New York; [4]Department of Pathology, Memorial Sloan Kettering Cancer Center, New York, New York; [5]Department of Epidemiology and Biostatistics, Memorial Sloan Kettering Cancer Center, New York, New York; [6]Molecular Pharmacology Program, Memorial Sloan Kettering Cancer Center, New York, New York; [7]Department of Radiology, Memorial Sloan Kettering Cancer Center, New York, New York; [8]Pharmacology Program, Weill Cornell Medical College, New York, New York; and [9]Department of Radiology, Weill Cornell Medicine, New York, New York

The presence of metastasis in local lymph nodes (LNs) is a key factor influencing choice of therapy and prognosis in cervical and endometrial cancers; therefore, the exploration of sentinel LNs (SLNs) is highly important. Currently, however, SLN mapping requires LN biopsy for pathologic evaluation, since there are no clinical imaging approaches that can identify tumor-positive LNs in early stages. Staging lymphadenectomy poses risks, such as leg lymphedema or lymphocyst formation. Furthermore, in 80%–90% of patients, the explored LNs are ultimately tumor-free, meaning most patients are unnecessarily subjected to lymphadenectomy. **Methods:** Current lymphoscintigraphy methods identify only the anatomic location of the SLNs and do not provide information on their tumor status. There are no noninvasive methods to reliably identify metastases in LNs before surgery. We have developed positron lymphography (PLG), a method to detect tumor-positive LNs, in which ^{18}F-FDG is injected interstitially into the uterine cervix on the day of surgery, and its rapid transport through the lymphatic vessels to the SLN is then visualized with dynamic PET/CT. We previously showed that PLG was able to identify metastatic LNs in animal models. Here, we present the first results from our pilot clinical trial (clinical trials identifier NCT02285192) in 23 patients with uterine or cervical cancer. On the morning of surgery, ^{18}F-FDG was injected into the cervix, followed by an immediate dynamic PET/CT scan of the pelvis and a delayed 1-h whole-body scan. **Results:** There were 3 (15%) node-positive cases on final pathologic analysis, and all of these LNs (including 1 with a focus of only 80 tumor cells) were identified by PLG. There were 2 (10%) false-positive cases with PLG, in which the final pathology of the corresponding SLNs was negative for tumor. **Conclusion:** This first-in-humans study of PLG in women with uterine and cervical cancer demonstrates its feasibility and its ability to identify patients with nodal metastases and warrants further evaluation in additional studies.

Received May 2, 2019; revision accepted Dec. 11, 2019.
For correspondence or reprints contact: Jan Grimm, Department of Radiology, Memorial Sloan Kettering Cancer Center, 1275 York Ave., New York, NY 10065.
E-mail: grimmj@mskcc.org
Published online Jan. 10, 2020.

Key Words: positron lymphography; sentinel lymph node; metastasis; PET; cervical cancer

J Nucl Med 2020; 61:1123–1130
DOI: 10.2967/jnumed.119.230714

Sentinel lymph node (SLN) mapping plays a central role in the detection of clinically relevant lymph nodes (LNs), replacing more invasive, less targeted approaches to nodal staging. The identification of the sentinel node or nodes—the primary draining LNs in a given malignancy—is now an established approach in the staging of tumors across a range of disease sites, and the technique has been adopted using various dyes, radiotracers, and imaging modalities. The concept of the SLN was first described in parotid gland cancer by Gould et al. in 1960 (*1*) and later explored more broadly in penile cancer by Cabanas et al. in the 1970s (*2*). SLN mapping and biopsy are now cornerstones of care and are performed routinely for apparent early-stage endometrial and cervical cancers (*3–9*).

Establishing nodal status is an important factor in patient management. The detection of a pathologically positive LN not only influences stage and prognosis in many cancers but also informs decisions on adjuvant treatment. Comprehensive LN dissection is not without attendant morbidity, however, and a significant number of patients who undergo lymphadenectomy experience disfiguring and painful leg lymphedema (*10*). These patients also incur intraoperative risk, including vascular and nerve injury and prolongation of operative time (*10–12*), as well as other concerns, which can include larger skin incisions, lymphocele formation, and impaired wound healing and risk of infection. SLN assessment is associated with much lower morbidity than comprehensive lymphadenectomy and is now an integral procedure in the staging and prognostication of many cancers, such as most endometrial and cervical malignancies (*3,6,13–16*), breast cancer (*17*), and melanoma (*18*).

Although nodal evaluation is important for prognostic assessment, risk stratification, and adjuvant treatment decisions, only

few SLNs are found to be positive for cancer. In a study of 266 patients with endometrial cancer at our institution, only 12% of SLNs were positive on final pathology (*6*). In a study of 2,001 patients with melanoma, only 21% had a positive SLN (*18*). In a study of patients with breast cancer, 41% had a positive SLN (*19*). Realizing the need for noninvasive technology to identify SLNs, several lymphography technologies have been developed. However, whereas all of these techniques will identify the SLN, none can reliably identify LNs that harbor metastases.

Lymphoscintigraphy with ^{99m}Tc-sulfur colloids, ^{99m}Tc-albumin colloids, or the recently approved ^{99m}Tc-Lymphoseek (^{99m}Tc-tilmanocept; Cardinal Health) (*20*), as well as vital blue or fluorescent dyes (indocyanine green [ICG] or fluorescein), are all nonspecific and can be used only to visualize an SLN, without providing any information on the tumor status of the node. Percutaneous optical imaging of ICG detected even fewer LNs than lymphoscintigraphy (*21*). Of critical concern is the potential for displacement of macrophages in SLNs by tumor cells, which can lead to a negative scan. Negative mapping with lymphography using ^{99m}Tc-sulfur colloid in patients with breast cancer has been associated with a higher number of tumor-positive SLNs not seen with lymphography but found on final pathology (*22*). The passage of these relatively large radiolabeled colloids can be blocked by tumor cells, thus limiting the clinical utility of this technique. Therefore, current methods do not accurately indicate the tumor status of the LN and, most alarmingly, may yield false-negative results.

PET imaging with intravenous ^{18}F-FDG has not improved the detection of micrometastases (metastatic deposits smaller than 2 mm) in LNs. ^{18}F-FDG PET imaging often fails to detect LN stations with metastases in normal-sized LNs in many cancers. For detecting metastases in normal-sized LNs, PET/CT had a sensitivity of only 17% in endometrial cancer (*23*), only 14% in melanoma (*24*), and only 48% in breast cancer (*19*). A recent study compared ^{18}F-FDG PET with diffusion-weighted imaging in patients with uterine cancers and concluded that neither diffusion-weighted imaging nor PET/CT was sufficiently accurate to replace lymphadenectomy. For small metastatic LNs, diffusion-weighted imaging and PET/CT showed a detection sensitivity of 75% and 16.7%, respectively (*25*). A metaanalysis showed that the overall accuracy of gadolinium-enhanced MRI for the detection of nodal metastases is only moderate as well (*26*).

Since micrometastasis in SLNs carries a significant negative prognostic value in many solid tumors, new imaging techniques to detect these relevant nodal metastases are urgently needed. To this end, we recently developed positron lymphography (PLG) (*27*). In PLG, ^{18}F-FDG is injected locally near or around the tumor and is then transported via the lymphatic channels to the draining SLN with a high signal-to-noise ratio, even in higher-echelon nodes, as was found in preclinical studies (*27*). We already demonstrated the feasibility of ^{18}F-FDG/PET imaging of the lymphatic system using intradermal ^{18}F-FDG injection in a healthy murine cohort, verifying both uptake in SLNs and the ability to use ^{18}F-FDG as a radiotracer (*27*). Our more recent work subsequently demonstrated the differential ^{18}F-FDG uptake in tumor-positive LNs versus normal SLNs in a melanoma murine model (*28*). Importantly, in dynamic studies, the uptake in tumor-positive LNs was significantly different from that in negative SLNs, allowing the identification of micrometastases (*29*). The small size of the tracer (e.g., glucose, 0.9 nm, compared with sulfur colloid, ~90 nm) allows passage through channels infiltrated with tumor cells, and the molecular function of the tracers allows their uptake by tumor cells, which is not achieved by any of the currently used colloid agents. And in contrast to PET with intravenous injection of the tracer, local injection in PLG ensures a high signal in the draining LNs, with little background signal anywhere else in the initial phase. This is particularly important in the pelvis, where high uptake in the bladder and bowel can obscure small LNs. PLG constitutes a new approach in lymphography, moving from current localization techniques to the characterization of SLNs based on molecular markers for cancer and lymphatic flow.

We hypothesized that PLG may provide more precise LN delineation, with minimal background signal, in the early phase of imaging and improve on conventional PET/CT and SLN mapping techniques to identify SLNs and delineate malignant from benign nodes. Our first-in-humans pilot study tested our hypothesis by expanding on an extensive body of work on the SLN biopsy technique and the rationale of using PLG as a primary modality. This involves a local, intracervical ^{18}F-FDG injection combined with PET/CT imaging. The primary goal of this pilot study was to evaluate the feasibility of intracervical injection of ^{18}F-FDG for PLG to identify SLNs and identify tumor-positive SLNs. The ability to do so would represent an invaluable new tool for surgeons performing SLN biopsy, providing them preoperatively with a 3-dimensional PET/CT map indicating the presence of tumor-positive nodes to be removed.

MATERIALS AND METHODS

Patient Selection

This prospective pilot study targeted enrollment of 20 evaluable patients for CT-based pelvic PLG on the day of their scheduled surgery for stage IB1 cervical cancer or staging surgery for high-grade endometrial cancer. Patients with high-grade endometrial tumors were selected in order to enrich for a higher proportion of occult LN-positive cases. Our protocol received institutional review board approval before patient enrollment, and all patients signed an informed consent form before participation (https://clinicaltrials.gov/ct2/show/NCT02285192). This protocol was deemed in compliance with the Health Insurance Portability and Accountability Act.

PLG

Intracervical ^{18}F-FDG applications are not routinely used in medical imaging; therefore, dosimetry curves were generated before the study and are provided in Supplemental Appendix 1 (supplemental materials are available at http://jnm.snmjournals.org). Based on calculated organ absorbed and effective dose estimates, a total dose range of 296–444 MBq (8–12 mCi) was administered to the cervix. The mean total dose injected was 426.9 MBq (11.5 mCi). Enrolled patients underwent intracervical injection of ^{18}F-FDG in the PET suite. With the patient already positioned on the scanner's table (GE Healthcare Discovery STE), a gynecologic oncologist inserted a speculum to visualize the intravaginal cervix and then ^{18}F-FDG was administered via syringe both superficially and deep to the face of the cervix at the 3- and 9-o'clock positions. Immediately after injection, dynamic PET/CT imaging (i.e., the PLG) of the pelvic region was obtained over 30 min (1 bed position, approximately from the aortic bifurcation to the symphysis) followed by a whole-body PET/CT acquisition performed as a 30-min (in the first few patients, 60 min) late-phase scan. Intravenous contrast medium was administered only for the pelvic CT to allow for better contrast in the pelvic PLG. The late-phase, whole-body scan was acquired as a standard PET/CT study with a reduced-dose, non–contrast-enhanced CT portion. Because the PLG was performed on the day of surgery, no oral contrast medium was applied.

Data collection included SUV and the anatomic location of pelvic and paraaortic LNs from PLG; all excised SLNs were evaluated perioperatively with a hand-held γ-probe. Intraoperative data, including the identification and anatomic location of pelvic and paraaortic SLNs, were also collected. Preoperative and intraoperative findings were correlated with postoperative pathologic findings in the SLNs.

Image Analysis

All analyses were performed immediately after imaging acquisition on a standard clinical GE Healthcare Centricity Workstation equipped with an Advantage Workstation analysis suite. The readers were board-certified nuclear medicine physicians, and 1 reader (JG) was board-certified in both radiology and nuclear medicine. Analysis of the dynamic series is not possible with the Advantage Workstation; therefore, 6 time points were extracted (every 5 min up to 30 min) and evaluated. The SUV_{max} was determined from nodes that were visible on early time points on the dynamic PET and then followed over time to visualize the course of uptake. At a later time point, a dedicated analysis of the dynamic study was performed using Hermes analysis software (Hermes Medical Solutions). The nodal SUVs of the dynamic study were fit to a decreasing monoexponential function to derive the time–activity curve of the individual LN. Any SLNs identified during the early analysis after PLG were recorded and communicated to the surgeons, with the intention of removal during the standard staging surgery on the day of PLG. Removal of an SLN was confirmed by measuring ex vivo radioactivity in the LN with a handheld positron probe (Node Seeker; Intra-Medical Imaging). On PLG, a suggestive LN was defined as any primary draining pelvic LN with a substantially sustained or increased SUV over time, relative to each patient's individual background. This was individualized to each patient and discussed with the surgeon for each case, as the SUVs reached values of several hundred in some patients but remained low in others, probably depending on variations in the injection.

Additional image reconstructions, showing the bones, vessels, and PET data as a maximum-intensity–rendered PET/CT overlay, were performed with the GE Healthcare PACS system, which was used to show the data to the surgical team. In addition, OsiriX (open-source licensing [lesser general public license]) was used for further visualization.

Surgery

After PLG, each patient underwent a standard staging surgery that included SLN mapping. The Gynecology Service within the Department of Surgery at Memorial Sloan Kettering Cancer Center uses an evidence-based standard algorithm for SLN mapping (Supplemental Appendix 2). This algorithm includes intracervical injection of vital blue dye or ICG for intraoperative fluorescent detection of SLNs. The uterine lymphatics take up the ICG, and patients map in 1 of 2 dominant patterns, with rare exceptions (Supplemental Appendix 3). The SLN is the first draining LN to take up colored dye. Any additional LNs that take up dye may be removed but are not considered SLNs. By adhering to these standard algorithms, the results of the PLG did not influence clinical decision making; removal of additional LNs suggestive on PLG but not considered SLNs was left to the surgeon's discretion.

If the PET imaging protocol identified SLNs other than those identified intraoperatively with dye, these LNs were removed in addition to the nodes identified by the standard algorithm. LN basins were defined in relation to vascular landmarks. These additional LNs removed were labeled as experimental LNs and were included in the tabulation of nodes considered discordant between the PET/CT and dye protocol. All LNs removed and identified as SLNs were subjected to the Clinical Laboratory Improvement Amendment–certified pathologic ultrastaging protocol, which is the standard at our institution for SLN pathologic assessment. Supplemental Appendix 4 details the pathologic ultrastaging protocol.

Analysis

Two detection methods were evaluated for accuracy in detecting SLNs: PLG and the clinical standard dye-assisted intraoperative SLN technique. Discordant SLNs were noted and descriptively reported. The primary endpoint at the nodal level was number of SLNs found using the dye technique and whether PLG was able to identify the same or additional SLNs. Successful mapping based on patient-level data was described as follows: the success rate of PLG as a mapping technique was compared with the conventional dye technique as our institutional gold standard to identify SLNs. Patients who mapped at least unilaterally were counted as having had successful mapping. Descriptive statistics were used to clarify the percentage unilateral versus percentage bilateral LN mapping and used to make rough success-rate comparisons (at the patient level) between the PLG and the dye-assisted intraoperative SLN mapping techniques.

To distinguish between tumor-positive and tumor-negative SLNs in women undergoing surgical staging for stage IB1 cervical cancer or high-grade endometrial cancer, we assessed SUV_{max} on dynamic-phase imaging during PLG and generated time–activity curves using ^{18}F-FDG uptake values over multiple time points. On the basis of our preclinical data (*28,29*), suggestive SLNs, that is, tumor-containing LNs, were expected to show a different uptake pattern from normal LNs, particularly a delayed peak or increasing uptake over time.

The SUV_{max} and the time to peak measured in individual LNs from the PLG were compared with the pathologic assessment (benign vs. malignant) of each labeled LN. An intraoperative γ-probe was used for an objective evaluation of the radioactivity and, most importantly, to confirm that the correct node with uptake was resected. Therefore, all experimentally identified SLNs were determined using objective measures.

Sensitivity at the level of nodal data was calculated for PLG. Exact specificity could not be determined, because a full LN dissection for endometrial and cervical cancers is no longer a standard surgical procedure at our institution and, therefore, the true-negative LN rate cannot be reported. As in all diagnostic testing, the goal is to maximize sensitivity without sacrificing specificity. In this study, maximizing sensitivity remains important, but without a full LN dissection we were unable to calculate the false-positive rate. The proportion of patients with at least 1 false-positive LN was reported.

Any possible adverse events associated with intracervical ^{18}F-FDG were also reported. We collected and reported data on demographic characteristics, surgical procedures performed, and intraoperative characteristics in a descriptive manner.

RESULTS

Twenty-three patients consented to undergo PLG. Two withdrew consent before undergoing PLG, and 1 patient's PLG scan was not assessable because of significant beam-hardening artifacts from a left hip prosthesis (patients 3, 4, and 12), leaving 20 patients evaluable for this study. The median age was 61 y (range, 26–81 y). The median body mass index (BMI) was 26.2 kg/m^2 (range, 20–42 kg/m^2). During surgery, 4 patients (20%) were administered isosulfan blue dye and 16 (80%) were administered ICG for intraoperative standard SLN mapping. Of the 20 patients undergoing PLG, 15 (75%) had endometrial and 5 (25%) had cervical cancer. All endometrial cancers were of high-grade histologic subtypes; the cervical tumors included 4 adenocarcinomas and 1 squamous cell carcinoma (Table 1). Of the 15 patients with endometrial cancer, 11 (73%) had stage I disease (uterus-confined) on final pathology. Of the 5 patients with cervical cancer, 4 (80%) had stage I disease (cervix confined) on final pathology.

TABLE 1
Characteristics of Patients Undergoing PLG After Intracervical ^{18}F-FDG Injection

Patient	Age (y)	BMI	Histology	Disease site	Dye used	PLG mapping			OR mapping			LNs removed (*n*)	Path-positive SLN	PLG-positive SLN
						Laterality	Right	Left	Laterality	Right	Left			
1	67	25	Carcinosarcoma	Uterus	Vital blue	Unilateral	Obturator		Bilateral	Obturator	External iliac	15	Right obturator	Obturator
2	81	41	Endometrioid	Uterus	ICG	Bilateral	External iliac	External iliac	Bilateral	External iliac	External iliac	3		
5	71	42	Serous	Uterus	ICG	Bilateral	External iliac/obturator	External iliac/obturator	Bilateral	Obturator	External iliac, obturator	6	Left and right obturator	Left obturator
6	67	26	Adenocarcinoma	Cervix	ICG	Bilateral	External iliac	External iliac	Bilateral	External iliac	External iliac	5		
7	57	31	Serous	Uterus	ICG	None			Bilateral	External iliac	External and internal iliac	4		
8	76	20	Carcinosarcoma	Uterus	ICG	Unilateral	External iliac		Bilateral	External iliac	External iliac	2		
9	51	21	Dedifferentiated	Uterus	ICG	None			Bilateral	External iliac, paraaortic	External iliac, obturator	5		
10	67	32	High-grade adenocarcinoma	Uterus	ICG	Bilateral	External iliac	External iliac	Bilateral	External iliac	Obturator	5		
11	47	31	High-grade adenocarcinoma	Uterus	ICG	Unilateral	External iliac		Bilateral	External iliac, obturator	External and internal iliac	4	No	Right external iliac
13	43	35	Adenocarcinoma	Cervix	ICG	Bilateral	External iliac	External iliac	Bilateral	External and internal iliac	External iliac	5		
14	40	23	Adenocarcinoma	Cervix	Vital blue	Bilateral	External iliac	External iliac	Bilateral	Internal iliac	External iliac, obturator	11	No	Right external iliac
15	61	24	Adenocarcinoma	Cervix	Vital blue	Unilateral	External iliac, obturator		Bilateral	External iliac, obturator	External iliac, internal iliac	6	Right obturator	Right external iliac/obturator
16	70	20	Carcinosarcoma	Uterus	ICG	Unilateral		Internal iliac	Bilateral	External iliac	External iliac	3		
17	60	28	Serous	Uterus	ICG	Unilateral		External iliac	Bilateral	External iliac	External iliac	5		
18	68	28	Serous	Uterus	ICG	None			Bilateral	Obturator	Obturator	5		
19	66	22	Endometrioid	Uterus	ICG	None			Bilateral	Internal iliac	External iliac, obturator	6		
20	26	21	Squamous cell carcinoma	Cervix	ICG	Bilateral	Internal iliac	Internal iliac, parametria	Bilateral	Internal iliac, obturator	Internal iliac, obturator	4		
21	61	26	Serous	Uterus	Vital blue	Unilateral		External iliac	None			0		
22	58	30	Endometrioid	Uterus	ICG	Bilateral	Common iliac	External iliac	Bilateral	Iliac bifurcation, obturator	Obturator	7		
23	54	27	Endometrioid	Uterus	ICG	Unilateral		Obturator	Bilateral	External Iliac	External iliac, obturator	12		

BMI = body mass index.

A median of 5 LNs was removed (range, 0–15 LNs) across all patients evaluated.

The median dose of ^{18}F-FDG injected into the cervix was 429.2 MBq (11.6 mCi) (range, 370.0–473.6 MBq [10.0–12.8 mCi]). Four patients had failed PLG mapping, and 1 patient did not undergo SLN removal at the time of surgery. There were 8 patients (40%) with bilateral and 8 (40%) with unilateral PLG mapping, for a combined successful mapping rate of 80%. One patient did not undergo SLN mapping in the operating room (OR), and of the 19 who mapped using the SLN dye technique in the OR, all 19 (100%) mapped bilaterally. There were 3 (15%) node-positive cases on final pathologic analysis, 2 endometrial and 1 cervical cancer, and 100% of these cases were detected by PLG. Among them was 1 with a focus of only 80 tumor cells within a single LN. There were 2 (10%) false-positive cases with PLG, suggesting positive SLNs and a final pathology finding of "negative for tumor" for the corresponding SLN. Table 1 summarizes demographic, disease, and imaging characteristics. There were no study-related adverse events noted for any of the 20 patients enrolled in the study.

True-Positive Cases

Three patients had true-positive SLNs detected by both PLG and SLN mapping, and these were confirmed on final pathology. As already observed in our preclinical study (*28,29*), ^{18}F-FDG uptake in tumor-positive LNs followed a pattern on the dynamic PLG different from that of benign LNs. Figure 1 demonstrates a representative patient with endometrial carcinosarcoma (stage IIIC1) who had unilateral PLG mapping on the right to 3 SLNs. Of the 3 LNs identified with PLG on the right, there was 1 right obturator SLN that demonstrated a delayed, prolonged ^{18}F-FDG uptake pattern with a late peak, as shown in the time–activity curve. This was different from the 2 additional SLNs seen on the right that demonstrated lower overall ^{18}F-FDG uptake with a benign uptake pattern, that is, an early peak and then rapid decline. The right obturator SLN seen on PLG with a unique uptake pattern corresponded to a right obturator SLN identified in the OR and was confirmed with ex vivo radioactivity measurement. Final pathology for this LN revealed 80 tumor cells within the node (Fig. 1; inset pathology photo). The patient did not map with PLG on the left side; however, a left external iliac SLN was identified and removed in the OR and found to be benign on final pathologic evaluation.

Patients 5 and 15 (Fig. 2) also had true-positive nodes as detected by both PLG and intraoperative SLN mapping, confirmed on final pathology. Patient 5 had serous endometrial cancer. Her PLG revealed a prolonged ^{18}F-FDG uptake that was only slowly decreasing over each time point. The PLG-positive SLN corresponded to a left obturator SLN in the OR, confirmed as radioactive with the handheld device on removal. Pathology revealed 2 micrometastatic foci measuring 2 and 3 mm in this node. A right external iliac or obturator PLG SLN was also identified using PLG; however, this node did not demonstrate any suggestive ^{18}F-FDG uptake and was interpreted as negative on PLG. This right-sided SLN was found to be positive, with an 11-mm tumor focus on final pathology. Patient 15 was diagnosed with a clinically

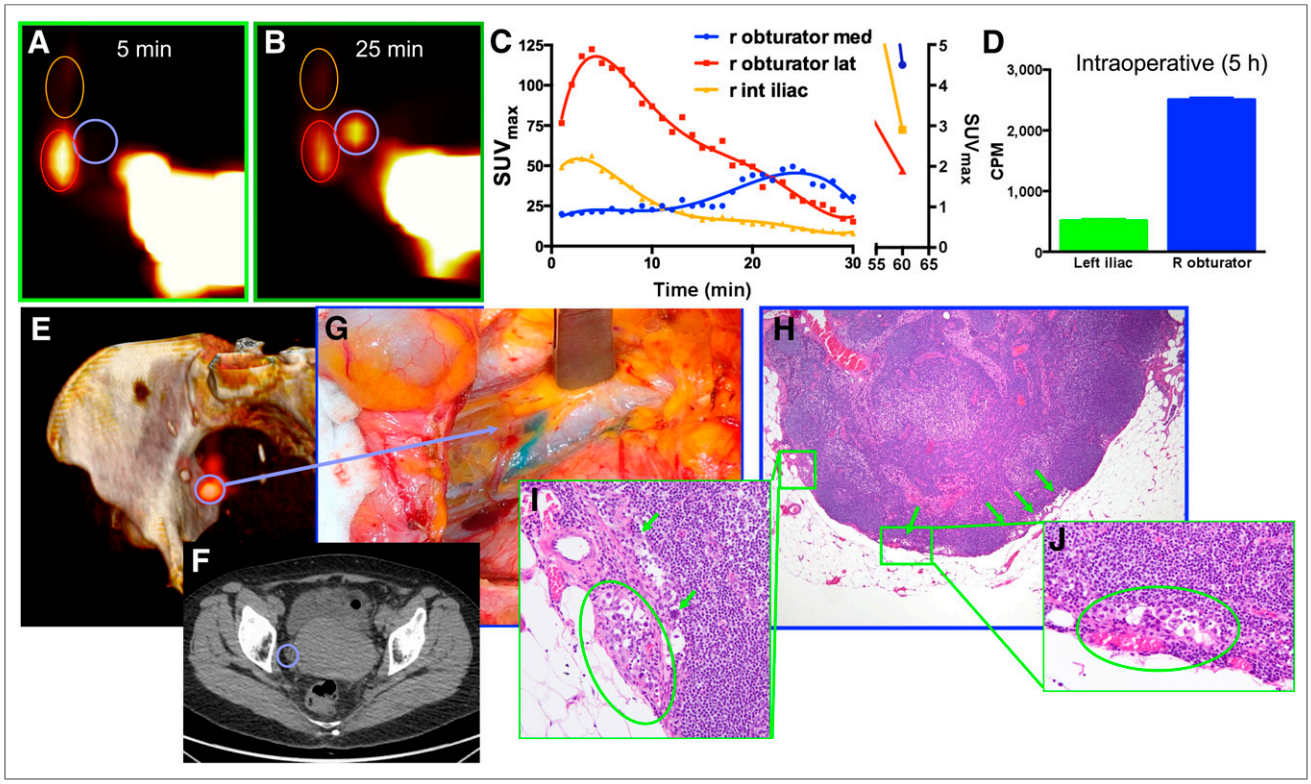

FIGURE 1. Representative example of clinical PLG with PET/CT and intracervical injection of ^{18}F-FDG in patient with uterine carcinosarcoma (patient 1). (A–C) PLG demonstrated 3 SLNs in right pelvis (A and B), 1 of which demonstrated a prolonged and delayed uptake pattern, as shown in time–activity curves (C). (D) Intraoperative measurements of counts per minute (CPM) of excised LNs demonstrated, even 5 h after tracer injection, higher uptake in suggestive node. (E and F) Three-dimensional surface reconstruction of PET/CT at 25 min showing higher uptake in suggestive node (blue circle, E) and same node as shown on axial CT (F). (G) Intraoperative view of node stained by vital blue dye. (H–J) Low-magnification (H) and high-magnification (I and J) histologic photomicrographs confirming presence of metastatic carcinoma within suggestive node.

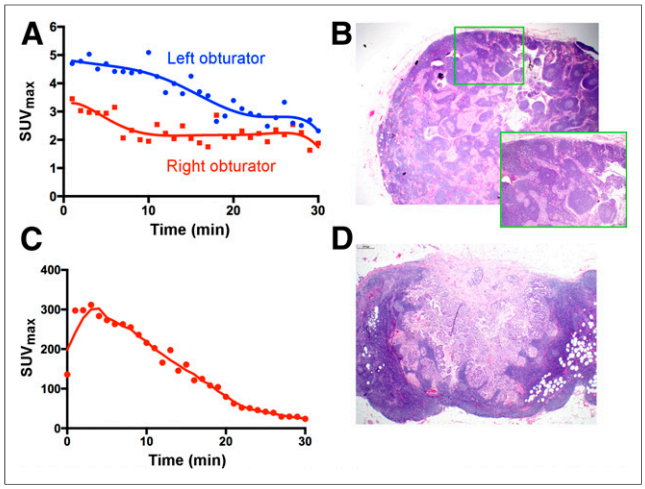

FIGURE 2. PLG of tumor-positive LNs. (A and B) Patient 5, with serous endometrial cancer, in whom time–activity curve of left obturator SLN demonstrated prolonged ^{18}F-FDG uptake in shoulder (A); this corresponded to left obturator SLN, which was removed in OR and revealed 2 micrometastatic tumor foci measuring 2 and 3 mm on final pathology (B). Right obturator PLG SLN was also identified and removed in OR. This node did not demonstrate prolonged uptake (or rapid decrease) on time–activity curve, was interpreted as negative on PLG, and was found to be positive on final pathology, with 11-mm metastatic tumor focus. (C and D) Patient 15, with stage IBI cervical adenocarcinoma, showing unilateral PLG mapping with delayed washout of ^{18}F-FDG from right external iliac/obturator SLN (C); this resected specimen contained 2 LNs, 1 of which was positive for tumor cells on final pathology (D).

stage IBI cervical adenocarcinoma. This patient demonstrated unilateral PLG mapping with prolonged ^{18}F-FDG uptake within a right external iliac or obturator SLN. This corresponded to a right obturator SLN. Final pathology revealed this excised specimen to contain 2 nodes, 1 of which was positive for tumor cells.

Micromorphometry of Nodes

We examined the micromorphometric features of each of the positive SLNs found in the study cohort. Each of the 3 cases exhibited distinct micromorphometric features. Patient 1 had a single positive SLN with a microscopic focus totaling approximately 80 tumor cells, consisting of multiple deposits of single cells and small clusters within a subcapsular sinus. Tumor deposits represented less than 1% of the total LN volume. Patient 5 had 2 positive SLNs identified, 1 of which was identified with PLG. The left obturator SLN revealed 2 micrometastatic tumor foci on pathologic evaluation. Micromorphometric analysis revealed a single tumor deposit occupying 60% of the LN, with an infiltrative, nodular pattern of tumor growth. The right obturator SLN was not seen with PLG, as there was no definite mapping to the side, and was described as an 11-mm tumor focus on pathologic evaluation. Micromorphometric evaluation revealed a single tumor deposit occupying 40% of the LN, with the same infiltrative, nodular pattern of tumor growth as seen in the contralateral SLN. Patient 15 had a single positive SLN on the right that occupied 15% of the LN and was a single deposit of tumor with an expansile, nodular pattern of tumor growth. Supplemental Appendices 5 and 6 provide complete micromorphometric descriptions and corresponding photographs.

Overall, all patients harboring positive nodes were identified. On the basis of the small number of positive LNs in this cohort, it is difficult to draw any correlation between morphology, tumor density in the node, and PLG results. A large cohort of node-positive patients will be required to better correlate PLG results with the morphometric characteristics of the positive nodes.

True-Negative Cases

Of the 20 evaluable patients in the PLG cohort, 11 (55%) underwent PLG and had a negative SLN both with PLG and with SLN mapping in the OR, as correlated with final pathologic evaluation. Four patients had failed mapping. Figures 3A and 3B highlight a negative case in which bilateral PLG mapping was observed, with nodes localizing to the external iliac nodal basins. On final pathology evaluation, these SLNs were negative for tumor.

False-Positive Cases

Two patients (patients 11 and 14) in the PLG cohort had positive SLNs seen on dynamic PET imaging. This positivity was based on the pattern of ^{18}F-FDG uptake seen in the SLN. Most representative was a patient with high-grade endometrial cancer (patient 11) showing unilateral PLG mapping and prolonged, increased ^{18}F-FDG uptake—with a delayed peak—within a right external iliac SLN suggestive of malignancy (Figs. 3C and 3D). This finding corresponded to a right external iliac SLN identified at the time of surgery (concordant mapping). Final pathology showed the SLN to be negative for tumor cells.

DISCUSSION

In this cohort of 20 patients, we have demonstrated the first-in-humans experience of PLG in endometrial and cervical cancer. Although this study was primarily for showing feasibility in a human cohort, we also sought to learn more about uptake patterns in tumor-positive and tumor-negative SLNs on PLG and to correlate this information with intraoperatively identified SLNs

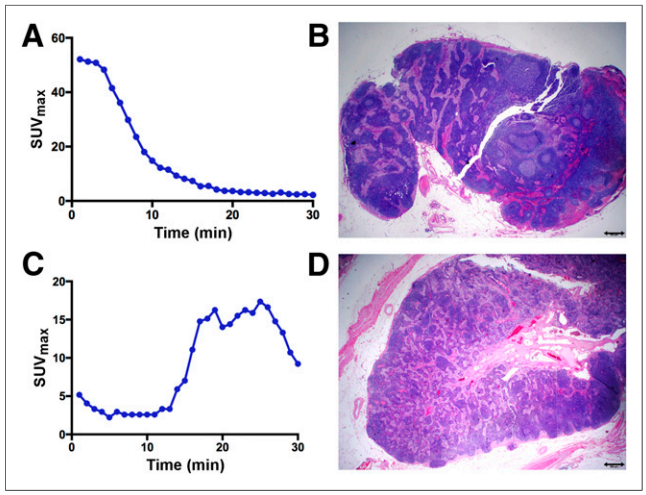

FIGURE 3. True-negative and false-positive PLG. (A and B) Patient 23 with high-grade endometroid adenocarcinoma and left obturator SLN that was negative on PLG (A) and pathology (B). (C and D) Patient 11, with high-grade endometrial cancer, showing unilateral PLG mapping with prolonged increase and delayed peak of ^{18}F-FDG uptake (C) within right external iliac SLN, which was suggestive of malignancy; this finding corresponded to right external iliac SLN at time of surgery (concordant mapping), but final pathology revealed this SLN to be negative for tumor cells (D).

and subsequent final pathology. We demonstrated the excellent sensitivity of this technique to identify tumor-positive LNs and also identified potential pitfalls that merit further evaluation and improvement. The number of reported false-positive cases (10%) was relatively high, in part because of the pattern of uptake seen in the PLG-identified nodes during dynamic-phase imaging, a pattern that was either equivocal (but not clearly benign) or most consistent with the pattern of a positive LN. We used our preclinical data to guide us on what constitutes normal versus suggestive uptake patterns in LNs. In our true-positive SLN cases, there was a common pattern of delayed, prolonged ^{18}F-FDG uptake in SLNs on dynamic-phase imaging that raised suspicion of malignancy. We also found that this feature was more subtle in some cases than in others. It is possible that with additional case experience, more than 1 positive uptake pattern may emerge.

A discussion and review of images immediately after PLG and before surgery allowed for the accurate localization and removal of the nodes seen on PLG. We encountered some challenges in identifying SLNs in certain locations, predominantly close to vessels and the ureters, due to a rapid transition of the injected ^{18}F-FDG into the circulation. This transition occurred much more quickly than in our preclinical setup, probably largely due to different injection sites (intracervical in humans vs. intracutaneous in mice). However, this is a commonly known limitation of ^{18}F-FDG use, as it is excreted quickly via the renal system. The use of intravenous contrast medium for the CT portion of PLG in the later cohort of patients partially helped to overcome this limitation. Given that most SLNs in cervical and endometrial cancer will be found in the obturator space, which is immediately adjacent to the ureter, alternative tracers that are more specific to tumor and not excreted in the urine should be explored. This is the subject of ongoing work in our group. It is also conceivable that PLG using a PET/MR scanner could enhance soft-tissue delineation, including genitourinary anatomy, and help overcome some of the challenges of a renally excreted radiotracer. Interestingly, the high activity at the cervical injection site was not a major limitation, mostly because most of the SLNs are found at the pelvic sidewall and not in the immediate vicinity of the cervix. However, there are potentially less complex anatomic sites in which PLG could be useful, such as in determining SLNs in breast cancer or melanoma.

We had initially allowed for 3 or fewer failed mapping cases in the first 10 patients evaluated before terminating our study for futility. We had 4 failed mappings in this study, with 2 in the first and 2 in the second set of 10 patients evaluated. Our initial estimate of successful mapping (at least unilateral) was set at 60% rather than 80% as with dye-based cervical injections, taking into account the experimental nature of this technique. A success rate of 80% mapping using PLG was noted, which was higher than anticipated and comparable to rates in the literature of SLN mapping using colored dye. Importantly, all surgeons performing injections for this study were experienced with the technique of cervical injections for SLN mapping. All but 1 patient in our cohort of 20 patients had successful bilateral mapping with ICG or vital blue dye. The 4 patients with failed mapping may be unique to the use of ^{18}F-FDG. More data are needed to better understand this finding.

CONCLUSION

PLG in patients with apparent early-stage cervical or endometrial cancer demonstrated 100% sensitivity in localizing positive SLNs. We report mapping success using ^{18}F-FDG in 80% of our cohort, a rate that is higher than anticipated. All patients with tumor-positive SLNs were correctly identified; however, some of the individual positive SLNs in those patients were missed. The limitations of PLG include the rapid transition of the ^{18}F-FDG into the circulation and subsequent rapid renal excretion, which can limit the localization of pelvic SLNs and lead to a high number (10%) of false-positive SLNs. Given the high sensitivity of this technique, further study is warranted, including the use of new tracers and improved imaging modalities to better visualize soft-tissue structures adjacent to nodes.

DISCLOSURE

Memorial Sloan Kettering Cancer Center is funded in part through NIH/NCI support grant P30 CA008748. Outside the submitted work, Nadeem Abu-Rustum has received grants from Stryker/Novadaq, Olympus, and GRAIL. No other potential conflict of interest relevant to this article was reported.

KEY POINTS

QUESTION: Is there a way to characterize, rather than just locate, SLNs in tumor patients to guide surgeons?

PERTINENT FINDINGS: In our pilot clinical trial, 20 patients with cervical or high-grade endometrial cancer were evaluated with the novel approach of PLG. All node-positive cases were correctly identified, including micrometastatic LNs, demonstrating feasibility and its ability to identify patients with nodal metastases.

IMPLICATIONS FOR PATIENT CARE: PLG could be a valuable tool to detect tumor-positive LNs before surgery and thus guide surgeons and limit complications from unnecessary lymphadenectomies.

REFERENCES

1. Gould EA, Winship T, Philbin PH, Kerr HH. Observations on a "sentinel node" in cancer of the parotid. *Cancer.* 1960;13:77–78.
2. Cabanas RM. An approach for the treatment of penile carcinoma. *Cancer.* 1977; 39:456–466.
3. Abu-Rustum NR. The increasing credibility of sentinel lymph node mapping in endometrial cancer. *Ann Surg Oncol.* 2013;20:353–354.
4. Abu-Rustum NR, Khoury-Collado F, Pandit-Taskar N, et al. Sentinel lymph node mapping for grade 1 endometrial cancer: is it the answer to the surgical staging dilemma? *Gynecol Oncol.* 2009;113:163–169.
5. Cibula D, Abu-Rustum NR, Dusek L, et al. Bilateral ultrastaging of sentinel lymph node in cervical cancer: lowering the false-negative rate and improving the detection of micrometastasis. *Gynecol Oncol.* 2012;127:462–466.
6. Khoury-Collado F, Murray MP, Hensley ML, et al. Sentinel lymph node mapping for endometrial cancer improves the detection of metastatic disease to regional lymph nodes. *Gynecol Oncol.* 2011;122:251–254.
7. Levenback CF, Ali S, Coleman RL, et al. Lymphatic mapping and sentinel lymph node biopsy in women with squamous cell carcinoma of the vulva: a gynecologic oncology group study. *J Clin Oncol.* 2012;30:3786–3791.
8. Rossi EC, Kowalski LD, Scalici J, et al. A comparison of sentinel lymph node biopsy to lymphadenectomy for endometrial cancer staging (FIRES trial): a multicentre, prospective, cohort study. *Lancet Oncol.* 2017;18:384–392.
9. Koh W-J, Abu-Rustum NR, Bean S, et al. Uterine neoplasms, version 1.2018: clinical practice guidelines in oncology. *J Natl Compr Canc Netw.* 2018;16:170–199.
10. Abu-Rustum NR, Alektiar K, Iasonos A, et al. The incidence of symptomatic lower-extremity lymphedema following treatment of uterine corpus malignancies: a 12-year experience at Memorial Sloan-Kettering Cancer Center. *Gynecol Oncol.* 2006;103:714–718.
11. Achouri A, Huchon C, Bats AS, Bensaid C, Nos C, Lecuru F. Complications of lymphadenectomy for gynecologic cancer. *Eur J Surg Oncol.* 2013;39:81–86.
12. Mariani A, Webb MJ, Keeney GL, Haddock MG, Calori G, Podratz KC. Low-risk corpus cancer: is lymphadenectomy or radiotherapy necessary? *Am J Obstet Gynecol.* 2000;182:1506–1519.

13. Barlin JN, Khoury-Collado F, Kim CH, et al. The importance of applying a sentinel lymph node mapping algorithm in endometrial cancer staging: beyond removal of blue nodes. *Gynecol Oncol.* 2012;125:531–535.
14. Burke TW, Levenback C, Tornos C, Morris M, Wharton JT, Gershenson DM. Intraabdominal lymphatic mapping to direct selective pelvic and paraaortic lymphadenectomy in women with high-risk endometrial cancer: results of a pilot study. *Gynecol Oncol.* 1996;62:169–173.
15. Cormier B, Diaz JP, Shih K, et al. Establishing a sentinel lymph node mapping algorithm for the treatment of early cervical cancer. *Gynecol Oncol.* 2011;122:275–280.
16. Levenback CF, van der Zee AG, Rob L, et al. Sentinel lymph node biopsy in patients with gynecologic cancers: expert panel statement from the International Sentinel Node Society Meeting, February 21, 2008. *Gynecol Oncol.* 2009;114:151–156.
17. Veronesi U, Paganelli G, Galimberti V, et al. Sentinel-node biopsy to avoid axillary dissection in breast cancer with clinically negative lymph-nodes. *Lancet.* 1997;349:1864–1867.
18. Morton DL, Thompson JF, Cochran AJ, et al. Final trial report of sentinel-node biopsy versus nodal observation in melanoma. *N Engl J Med.* 2014;370:599–609.
19. Song BI, Kim HW, Won KS. Predictive value of ^{18}F-FDG PET/CT for axillary lymph node metastasis in invasive ductal breast cancer. *Ann Surg Oncol.* 2017; 24:2174–2181.
20. Baker JL, Pu M, Tokin CA, et al. Comparison of [^{99m}Tc]tilmanocept and filtered [^{99m}Tc]sulfur colloid for identification of SLNs in breast cancer patients. *Ann Surg Oncol.* 2015;22:40–45.
21. Namikawa K, Tsutsumida A, Tanaka R, Kato J, Yamazaki N. Limitation of indocyanine green fluorescence in identifying sentinel lymph node prior to skin incision in cutaneous melanoma. *Int J Clin Oncol.* 2014;19:198–203.
22. Brenot-Rossi I, Houvenaeghel G, Jacquemier J, et al. Nonvisualization of axillary sentinel node during lymphoscintigraphy: is there a pathologic significance in breast cancer? *J Nucl Med.* 2003;44:1232–1237.
23. Kitajima K, Murakami K, Yamasaki E, et al. Accuracy of ^{18}F-FDG PET/CT in detecting pelvic and paraaortic lymph node metastasis in patients with endometrial cancer. *AJR.* 2008;190:1652–1658.
24. Singh B, Ezziddin S, Palmedo H, et al. Preoperative ^{18}F-FDG-PET/CT imaging and sentinel node biopsy in the detection of regional lymph node metastases in malignant melanoma. *Melanoma Res.* 2008;18:346–352.
25. Kitajima K, Yamasaki E, Kaji Y, Murakami K, Sugimura K. Comparison of DWI and PET/CT in evaluation of lymph node metastasis in uterine cancer. *World J Radiol.* 2012;4:207–214.
26. Klerkx WM, Heintz AP, Mali WP, et al. Lymph node detection by MRI before and after a systematic pelvic lymphadenectomy. *Gynecol Oncol.* 2009;114:315–318.
27. Thorek DL, Abou DS, Beattie BJ, et al. Positron lymphography: multimodal, high-resolution, dynamic mapping and resection of lymph nodes after intradermal injection of 18F-FDG. *J Nucl Med.* 2012;53:1438–1445.
28. Lockau H, Neuschmelting V, Ogirala A, Vilaseca A, Grimm J. Dynamic ^{18}F-FDG PET lymphography for in vivo identification of lymph node metastases in murine melanoma. *J Nucl Med.* 2018;59:210–215.
29. Morton DL, Thompson JF, Essner R, et al. Validation of the accuracy of intraoperative lymphatic mapping and sentinel lymphadenectomy for early-stage melanoma: a multicenter trial. Multicenter Selective Lymphadenectomy Trial Group. *Ann Surg.* 1999;230:453–463.